Carbohydrate Polymers 86 (2011) 1410–1416

Contents lists available at ScienceDirect

Carbohydrate Polymers

journal homepage: www.elsevier.com/locate/carbpol

Electrospinning β-cyclodextrin/poly(vinyl alcohol) nanofibrous membrane for molecular capture

Wang Zhang, Ming Chen, Guowang Diao*

College of Chemistry and Chemical Engineering, Yangzhou University, Yangzhou, 225002 Jiangsu, PR China

ARTICLE INFO

Article history:
Received 28 April 2011
Received in revised form 12 June 2011
Accepted 21 June 2011
Available online 29 June 2011

Keywords:
Electrospinning
β-Cyclodextrin
Poly(vinyl alcohol)
Molecular capture
Functional nanofiber

ABSTRACT

A novel β-cyclodextrin/poly(vinyl alcohol) nanofibrous membrane (β-CD/PVA_{nfm}) with the function of molecular capture was successfully prepared by electrospinning homogeneous aqueous solutions of β-CD and PVA. β-CD/PVA_{nfm} was characterized by scanning electronic microscopy and Fourier transform infrared spectroscopy. The viscosity of β-CD/PVA solution was increased with the concentration of β-CD and high viscosity of β-CD/PVA solution was beneficial to form more uniform nanofibers. The interaction between β-CD and PVA in the solution was studied by rheological measure and ^{1}H NMR spectra. The rheological change of electrospinning solutions was attributed to the intermolecular hydrogen bonding between β-CD and PVA in the solution, which was confirmed by ^{1}H NMR spectra. The electrochemical measurement showed that β-CD/PVA_{nfm} could recognize small hydrophobic molecules such as ferrocene (Fc) by forming inclusion complexes. The molecular capturing ability of β-CD/PVA_{nfm} was increased with the amount of β-CD in composite nanofibrous membrane. The results suggested that the composite nanofibrous membrane was potentially applied to purification/separation processes, electrochemical sensor, drug delivery, and so on.

1. Introduction

β-Cyclodextrin (β-CD) is a cyclic oligosaccharide including seven glucose unites linked by α-1,4-glucosidic bonds. Its special molecular structure – hydrophobic internal cavity and hydrophilic external surface can form non-covalent host–guest complexes with a variety of molecules (Szejtli, 1998). Furthermore, β-CD is an excellent model of enzymes, which leads to its use as catalysts, both in enzymatic and nonenzymatic reactions, and it is a natural product and readily available for most researchers (Li & Purdy, 1992). Since the distinct physical and chemical properties of inclusion complexes can be tailored by β-CD inclusion complexes, β-CD is used in many fields, such as pharmaceuticals (Namazi & Kanani, 2009), foodstuff (Yang, Gu, Xu, Li, & Zhang, 2010), separate technique (Zhao, Lin, Wang, & Yao, 2010), environmental protection (Jozefaciuk, Muranyi, & Fenyvesi, 2003) and genetic engineering (Xu et al., 2009).

Electrospinning is a versatile technique for producing multifunctional nanofibers from various polymers, polymer blends and composites (Greiner & Wendorff, 2007; Li & Xia, 2004). Electrospinning nanofibers have many unique properties such as high surface area-to-volume, pore size within a nano range, high porosity and flexibility for chemical/physical functionalization (Reneker & Yarin, 2008). Therefore, it has been shown that the very fascinating properties of these electrospun nanofibers make them applicable in numerous areas, including biotechnology (Jia et al., 2007), membranes/filters (Wang et al., 2005), electroanalysis (Shan et al., 2010), power source (Yu, Gu, Zhu, Aken, & Maier, 2009), and so on. However, most of the electrospinning nanofibers cannot capture organic molecules or heavy metal ions. Simple nanofibers containing β-CD will, therefore, gain special characteristics, which outstandingly develop and extend the practical application areas of nanofibers. On the one hand, nanofibrous membranes consisting of β-CD can be used for the separation of industrial waste, since they have large surface area along with a nano-porous structure (Barhate & Ramakrishna, 2007). On the other hand, β-CD can capture molecules for removing the polluting substances from the environment by forming inclusion complexation (Chen, Diao, & Zhang, 2006).

Up to date, some studies focus on the morphology improvement of electrospinning nanofibers with cyclodextrins (Uyar, Balan, Toppare, & Besenbacher, 2009; Uyar, Kingshott, & Besenbacher, 2008), but very few researchers take into account of the ability of composite nanofibers for capturing guest molecules. In this paper, β-CD/PVA_{nfm} was prepared by electrospinning. In the study of rheological behavior and ^{1}H NMR spectra of β-CD/PVA solutions, the

* Corresponding author. Tel.: +86 514 87975436; fax: +86 514 87975244.
E-mail address: gwdiao@yzu.edu.cn (G. Diao).

0144-8617/$ – see front matter © 2011 Elsevier Ltd. All rights reserved.
doi:10.1016/j.carbpol.2011.06.062

influence of β-CD in electrospinning solutions was explained by the intermolecular interaction between β-CD and PVA due to the formation of hydrogen bond causing the enhancement of the viscosity of electrospinning solution with β-CD present. The ability of β-CD/PVA_{nfm} for capturing guest molecules was researched by cyclic voltammetry with Fc as a model of guest molecules. Our attention was focused to unearth the relationship between β-CD and PVA responsible for the improvement of the morphology of electrospinning nanofiber, and found a good model system for studying the effect of capturing molecules, thus contributing to the use of β-CD functional materials in purification/separation processes.

2. Experimental

Poly(vinyl alcohol) (PVA) with 1750 ± 50 degree of polymerization and 98% degree of hydrolysis, β-cyclodextrin (β-CD), ferrocene (Fc) and other reagents were purchased from Shanghai Chemical Reagents Company (China). Double distilled and sterilized water was used to prepare all solutions.

The solutions used for electrospinning were prepared by dissolving PVA and β-CD/PVA in water at 90 °C under stirring for 2 h. The concentration of PVA was 8 wt.%. The amount of β-CD was 0 wt.%, 10 wt.%, 20 wt.%, 3.0 wt%, 40 wt.% with respect to PVA. Above polymer solution was put into a 10 ml plastic syringe fitted with a metallic needle of 1.2 mm inner diameter. The syringe was fixed horizontally with a syringe pump (Baoding longer, LSP01-1A) and the electrode of the high voltage power supply (Tianjin Dongwen, DWLP303-1ACDB) was connected to the metal needle tip. The working distance between the needle tip and the ground electrode was 15 cm. The solution flow rate was 1.5 ml/h. The electrospinning voltage was 27 kV. The electrospinning temperature and the relative humidity were 25 °C and 50%, respectively.

The SEM images of nanofibers deposited on aurum foils were measured on a FE-SEM instrument (Hitachi, S-4800). The nanofibrous membranes were analyzed by the FTIR spectrophotometer (Bruker, Tensor 27). The ^{1}H NMR spectra were conducted on a 600 MHz Bruker spectrometer (Bruker, Germany) at 303.1 K in DMSO. The viscosity of the solution was measured at 25 °C using the rheometer (Thermo, RS600) which was equipped with a cone accessory.

The capturing ability of β-CD/PVA_{nfm} to guest molecules was measured as follows: firstly, the PVA_{nfm} and β-CD/PVA_{nfm} with different amount of β-CD (0, 10, 20, 30, and 40 wt.% with respect to PVA; the mass of nanofiber on the electrode: 0.3 mg) were electrospun on a surface of glassy carbon electrode (GCE, diameter: 3 mm), respectively. The process was shown in Scheme 1. Secondly, the nanofibers modified electrodes were immerged in Fc/ethanol saturated solution for 10 min. The modified electrodes were washed with ethanol to remove residual Fc on the modified electrode. Then the modified electrode was dried in room temperature for 1 h. All eletrochemical experiments were performed on an electrochemical work station (Shanghai Chenhua, CHI660a) equipped with a three-electrode jacked cell. A GCE was served as a working electrode. Reference and counter electrodes were saturated calomel electrode (SCE) and platinum wire electrode, respectively. All experiments were carried out at 25 °C in 0.1 M phosphate buffer solution (pH 6.8).

3. Results and discussion

3.1. Characterization of electrospinning nanofibrous membranes

Fig. 1 presented SEM images of electrospinning nanofibrous membranes obtained by electrospinning polymer solutions contained 8 wt.% PVA and different amount of β-CD, such as 0, 10, 20, 30 and 40 wt.% (with respect to PVA). In Fig. 1(a), there were many beads on the nanofibrous membrane of PVA. However, compared with pure PVA_{nfm}, the morphology of nanofibers could be adjusted by β-CD at a given amount of PVA in Fig. 1(b)–(e). With the amount of β-CD increased from 10 to 40 wt.%, not only the number of beads in β-CD/PVA_{nfm} was decreased, but also the bulk of the shuttle-shape beads in β-CD/PVA_{nfm} was smaller than that in PVA_{nfm}. At last, while the concentration of β-CD increased to 40 wt.%, uniform nanofibers were obtained. This change of the morphology of nanofibers was similar to that of β-CD/PMMA system reported in reference Uyar et al. (2009). The average diameters of nanofibers (ADF) in both PVA_{nfm} and β-CD/PVA_{nfm} were calculated and summarized in Fig. 1(f). It was shown that the ADF of β-CD/PVA_{nfm} increased with the concentration of β-CD, which suggested the relationship between the ADF and the concentration of β-CD. The results of SEM images showed that β-CD in the electrospinning composite nanofibrous membrane played a positively effective role in changing the morphology of nanofibers.

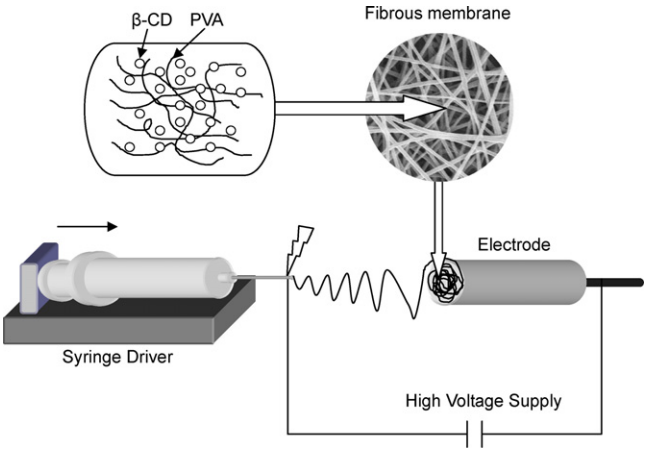

Scheme 1. The preparation of β-CD/PVA_{nfm} modified electrode.

FTIR spectra for β-CD, PVA_{nfm} and β-CD/PVA_{nfm} were shown in Fig. 2. The typical bands of β-CD were exhibited in Fig. 2(a). The bands observed at 3382, 2926 and 1029 cm^{-1} were assigned to stretching vibration of –OH, CH/CH_2 and the coupled C–C/C–O, respectively. For PVA, the characteristic vibration peaks of –OH at 3421 cm^{-1}, stretching vibrations of CH and CH_2 groups at 2800–3000 cm^{-1}, deformation vibrations of CH/CH_2 at 1250–1500 cm^{-1}, C–O stretching vibration at 1093 cm^{-1} were clearly appeared in Fig. 2(b). The absorption bands of β-CD/PVA nanofibers at different wt.% of β-CD in Fig. 2(c)–(f) were similar to those of PVA nanofibers. However, the band at about 1030 cm^{-1} was shown in the FTIR spectra of β-CD/PVA_{nfm} corresponded to the coupled C–C/C–O stretching vibrations of β-CD, which proved that β-CD molecules existed in β-CD/PVA_{nfm}. It was also found that the absorption peak at about 3450 cm^{-1} assigned to –OH stretching vibrations became stronger with the increase of β-CD in the electrospun blends.

3.2. Rheological properties of electrospinning solutions

In the electrospinning process, the viscosity of solutions was a very important parameter for the formation of fiber (Greiner & Wendorff, 2007). In order to understand the dependence of the viscosity of electrospinning solutions with β-CD, the rheological properties of PVA and β-CD/PVA solutions were studied. Fig. 3(A) showed the shear rate dependence of viscosity for a 8 wt.% PVA solution containing a different amount of β-CD. PVA solution without β-CD in curve (a) was electrostatically stabilized

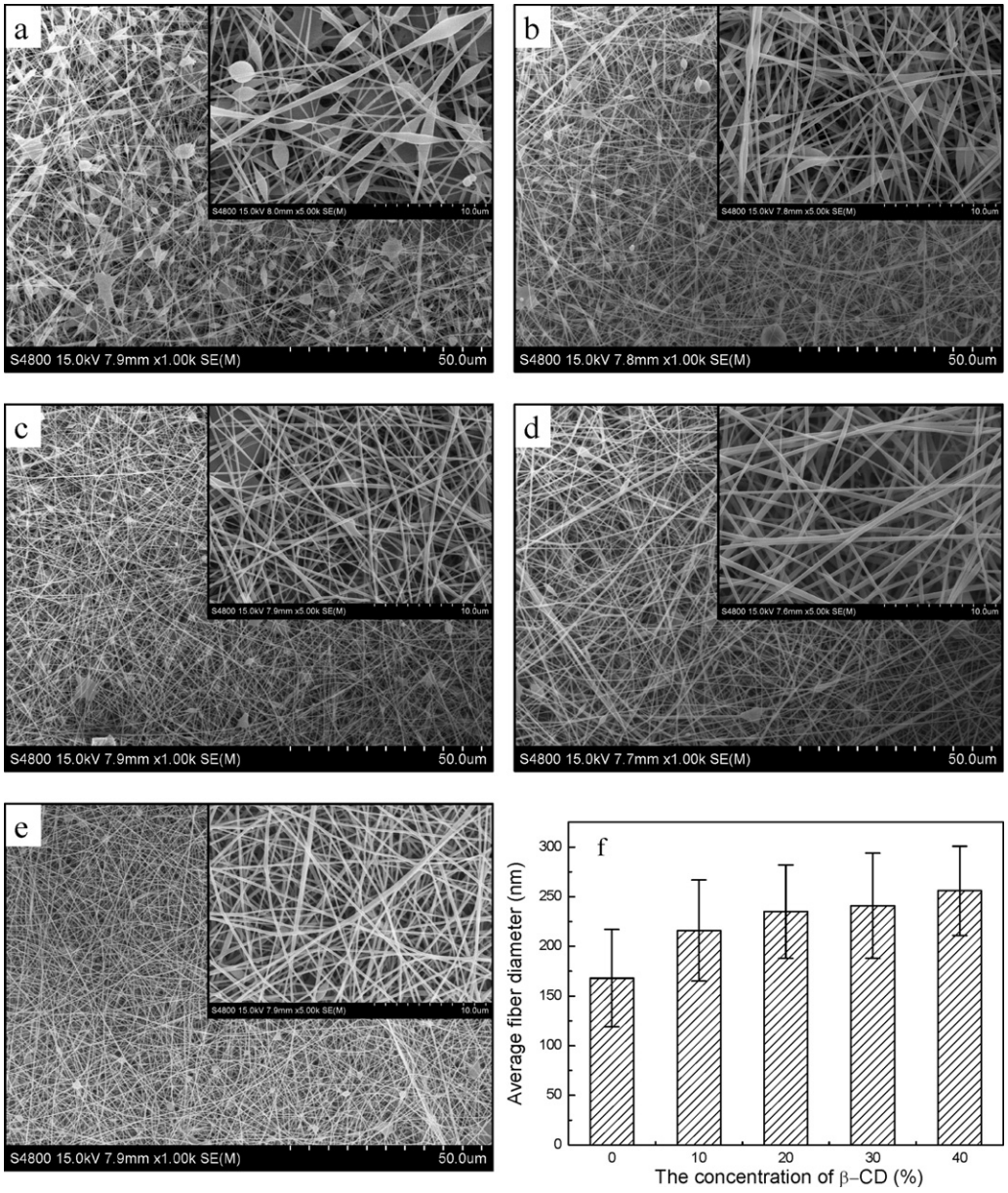

Fig. 1. SEM images of electrospinning nanofibers from 8 wt.% PVA solutions at different wt.% of β-CD with respect to PVA: (a) 0 wt.%, (b) 10 wt.%, (c) 20 wt.%, (d) 30 wt.%, (e) 40 wt.%, the insets showed higher magnification images. (f) Average fiber diameter of electrospinning nanofibers with the different ratios of β-CD from 0 wt.% to 40 wt.%.

and Newtonian with a viscosity of 0.2363 Pa s, which was close to the value reported in reference Otsubo (1995). From curve (b) to curve (e), the addition of β-CD caused the viscosity increasing over the entire range of shear rates. As the β-CD concentration increased, the effect of β-CD became gradually more prominent. The increase of the viscosity at a given amount of PVA with the amount of β-CD monomer could be ascribed to the strong intermolecular interaction between PVA and β-CD. Furthermore, the significant shear-thinning effect was found with the addition of β-CD at low shear rates. The shear-thinning flow could be explained by the shear-induced breakdown of the intermolecular junctions which was formed by the entangled PVA polymer chains and β-CD molecules in β-CD/PVA solution. When the shear rate exceeded 50 s^{-1}, the flow characteristic changed from shear-thinning to Newtonian. It should be pointed out that the transition was probably due to stretching and alignment of the polymer chains at a high shear rate and thereby the association network between PVA and β-CD could not be reformed, resulting in a similar Newtonian flow to PVA solution. This was possibly due to the intermolecular interactions between β-CD and PVA resulted in high viscosity of β-CD/PVA solution and therefore let uniform fibers with fewer beads form in the electrospinning process (as shown in Fig. 1).

In Fig. 3(B), the viscosity of electrospinning solution was plotted as a function of the concentration of β-CD. The viscosity of β-CD/PVA solution was higher than that of PVA solution, and the viscosity of β-CD/PVA solution also increased with the concentration of β-CD in PVA. The high viscosity of β-CD/PVA solution resulted in the less numbers of beaded fibers and the larger average diameter, which was similar to the correlation between polymer solution viscosity and the electrospinning fibrous morphology (Fong, Chun, & Reneker, 1999).

3.3. Intermolecular interaction between β-CD and PVA

In order to confirm the intermolecular interaction between β-CD and PVA, ^{1}H NMR spectra of β-CD, PVA, and β-CD/PVA were

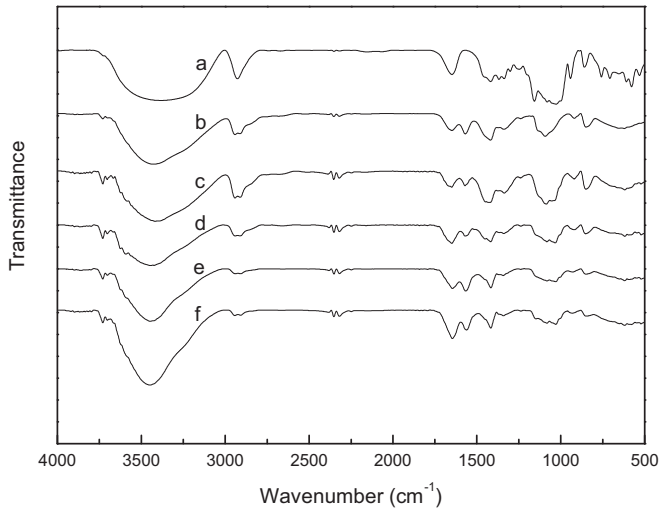

Fig. 2. FTIR spectra of (a) β-CD and electrospinning nanofibers from 8 wt.% PVA solutions at different wt.% of β-CD with respect to PVA: (b) 0 wt.%, (c) 10 wt.%, (d) 20 wt.%, (e) 30 wt.%, (f) 40 wt.%.

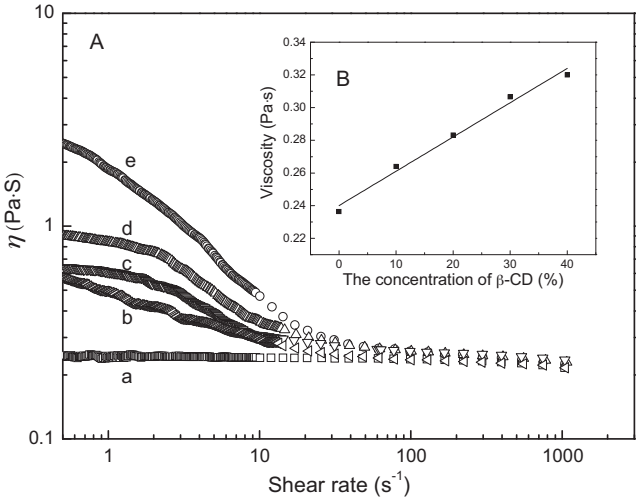

Fig. 3. (A) Shear rate dependence of viscosity for suspensions in 8 wt.% PVA solutions containing β-CD at different concentrations: (a) 0 wt.%, (b) 10 wt.%, (c) 20 wt.%, (d) 30 wt.%, (e) 40 wt.%. (B) The viscosity of electrospinning solution as a function of β-CD concentration. Date taken from (A).

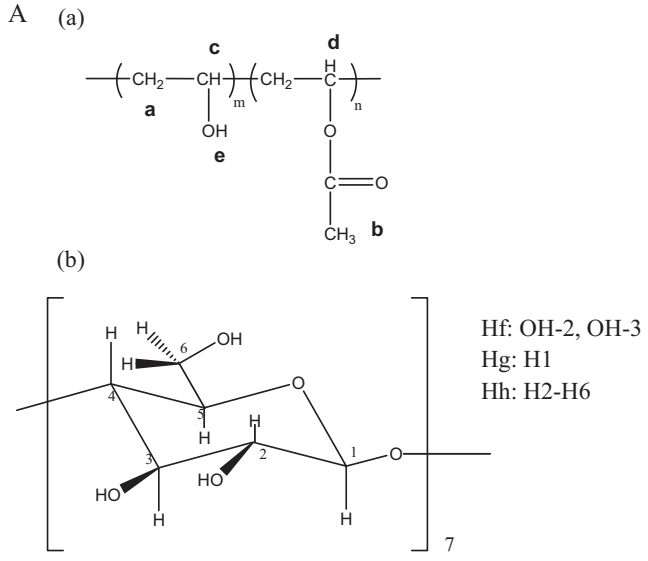

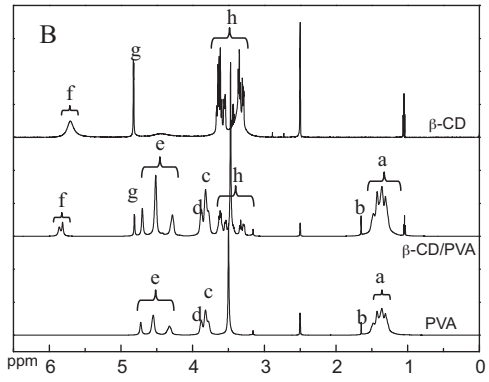

Fig. 4. (A) The chemical structures of (a) PVA and (b) β-CD. (B) ^{1}H NMR spectra of β-CD, PVA, and β-CD/PVA (β-CD, 30 wt.%).

measured. Fig. 4(A) showed the chemical structure of (a) PVA and (b) β-CD, and Fig. 4(B) showed the ^{1}H NMR spectra of β-CD, PVA, and β-CD/PVA. The values of chemical shifts, δ for different protons in β-CD, PVA, and β-CD/PVA were listed in Table 1, where the hydrogen atoms were labeled in Fig. 4(A). For pure PVA, it was often synthesized by hydrolysis of poly(vinyl acetate) (PVAc), therefore, some chemical structure of PVAc was kept in PVA. From the ^{1}H NMR spectra of PVA in DMSO, the chemical shifts of methylene protons (Ha) appeared at 1.30–1.50 ppm and the methine protons (Hc and Hd) attached to –OH and –$OCOCH_3$ appeared at 3.82 and 3.88 ppm, respectively. The –CH_3 protons (Hb) of the acetate group were at 1.65 ppm. The hydroxyl protons (He) of PVA were separated into characteristic triads at 4.33/4.55/4.72 ppm due to the hydrogen bonding between –OH groups of the polymer and DMSO (Gholap, Jog, & Badiger, 2004).

The ^{1}H NMR spectrum of β-CD/PVA with 30 wt.% β-CD in DMSO was shown in Fig. 4(B). Most of the peaks (Ha, Hb, Hc, and Hd), which had appeared in pure PVA, also appeared in β-CD/PVA in the same chemical shift values. Furthermore, the typical chemical shifts for β-CD protons (Hg and Hh) in β-CD/PVA were observed, which was in agreement with the ^{1}H NMR spectrum of β-CD in Fig. 4(B). However, compared with the chemical shifts of protons in pure PVA, only the hydroxyl protons (He) of PVA in β-CD/PVA appeared a little change and was shifted to upfield, which indicated that the micro-environment of the hydroxyl of PVA in β-CD/PVA was different from that in pure PVA. On the other hand, β-CD/PVA presented several extra chemical shifts appearing at 5.82 and 5.86 ppm (Hf), corresponding to the proton signals of β-CD hydroxyl groups. Compared with the hydroxyl protons (Hf) of native β-CD at δ = 5.70 in Fig. 4(B), hydroxyl resonance of β-CD in β-CD/PVA solution appeared a small splitting and was shifted to the downfield direction. These results could be interpreted as a consequence of hydrogen bonding interaction between PVA and β-CD in β-CD/PVA solution. It was meant that the intermolecular interaction between β-CD and PVA was attributed to hydrogen bonding, and therefore the β-CD/PVA solution exhibited the particular rheology and high viscosity, which was propitious to obtain the uniform nanofibers by electrospinning.

3.4. Molecular recognition of β-CD/PVA$_{nfm}$

To confirm the capturing ability of β-CD/PVA$_{nfm}$ for the guest molecule, Fc was investigated by cyclic voltammetry (CV). Fig. 5(A)

Table 1
Chemical shifts for ^{1}H NMR spectra of PVA, β-CD/PVA and β-CD.

	δ (ppm)							
	a	*b*	*c*	*d*	*e*	*f*	*g*	*h*
PVA	1.30–1.50	1.65	3.82	3.88	4.33/4.55/4.72			
β-CD/PVA	1.30–1.50	1.65	3.82	3.88	4.28/4.52/4.70	5.86/5.82	4.81	3.00–3.70
β-CD						5.70	4.83	3.00–3.70

showed the voltammogram of Fc absorbed on a electrode modified by β-CD/PVA_{nfm} with different amount of β-CD, such as 0, 10, 20, 30 and 40 wt.%, in 0.1 M PBS (pH 6.8) at 25 °C with a scan rate of 100 mV s^{-1}. In curve (a), there was no electrochemical redox of Fc for an electrode modified by pure PVA_{nfm}, which indicated that PVA_{nfm} cannot capture the guest molecule. However, curve (b) exhibited a couple of stable and well-defined redox peaks, which indicated that Fc was successfully captured by β-CD/PVA_{nfm} modified on the electrode by forming inclusion complex between Fc and β-CD in β-CD/PVA_{nfm}. The anodic peak potential (E_{pa}) and cathodic peak potential (E_{pc}) were located at +0.239 and +0.146 V, respectively. The separation between E_{pa} and E_{pc} (ΔE_p) was 93 mV, which was close to the value of Fc-β-CD reported in reference Matsue, Evans, Osa, and Kobayashi (1985). Furthermore, it was found that the cathodic peak current i_{pc} increased with the amount of β-CD in β-CD/PVA_{nfm} modified on the electrode (curves (b)–(e) in Fig. 5(A)), and the relationship of i_{pc} and the amount of β-CD in β-CD/PVA_{nfm} was shown in Fig. 5(B). A good linearity suggested that the more amount of β-CD in β-CD/PVA_{nfm} was, the more Fc would be captured by the modified electrode, which further confirmed that the adsorption of Fc on the modified electrode was due to the capture of β-CD in β-CD/PVA_{nfm}. The anodic peak potential, E_{pc} of the modified electrode, moreover, shifted in the more positive direction with the more addition of β-CD, which was attributed to the steric hindrance of the inclusion complexes. However, the anodic current was lower than the cathodic current, and an interesting feature was the trend of the anodic current wave to exhibit a plateau rather than a peak from curve (b) to (e), which was similar to the literature (Buriez et al., 2008).

Fig. 5(C) showed the multi-cyclic voltammograms of Fc absorbed onto β-CD/PVA_{nfm} with 10% β-CD modified electrode in PBS. The current was almost unchanged in different cycles, which confirmed that the stability of the Fc/β-CD/PVA_{nfm} modified electrode was quite outstanding. The excellent stability was attributed to the formation of inclusion complexes between Fc and β-CD, which could effectively prevent the leakage of a mediator from the modified electrode. Therefore, the good capturing ability for Fc as a mediator for electron transfer could be used in electrochemical sensors or biosensors.

Fig. 6 showed the SEM images of the β-CD/PVA_{nfm} (30 wt.% β-CD) modified electrode before (a1 and a2) and after capturing the Fc (b1 and b2). In comparison with Fig. 6(a1), the resulting nanofibrous modified electrode after capturing the Fc still retained the overall morphology, and did not show distinguishable variations of fibrous size in Fig. 6(b1), which revealed that the molecular capturing process hardly damaged the morphology of nanofibers. It was, therefore, important to note that the dimension stability of the nanofibers facilitate the recycled use of the modified electrode. On the other hand, Fig. 6(a2) showed the modified electrode before capturing the Fc with the high magnification. The surface of PVA/β-CD nanofibers on the modified electrode was rather smooth and uniform. After capturing the Fc, however, the surface of the nanofiber became rougher in Fig. 6(b2). The increase of the surface roughness of nanofibers suggested that the inclusion complexes of Fc with β-CD formed on the nanofibrous surface, which indicated the capturing ability of β-CD/PVA_{nfm} for the guest molecule from indirect sources.

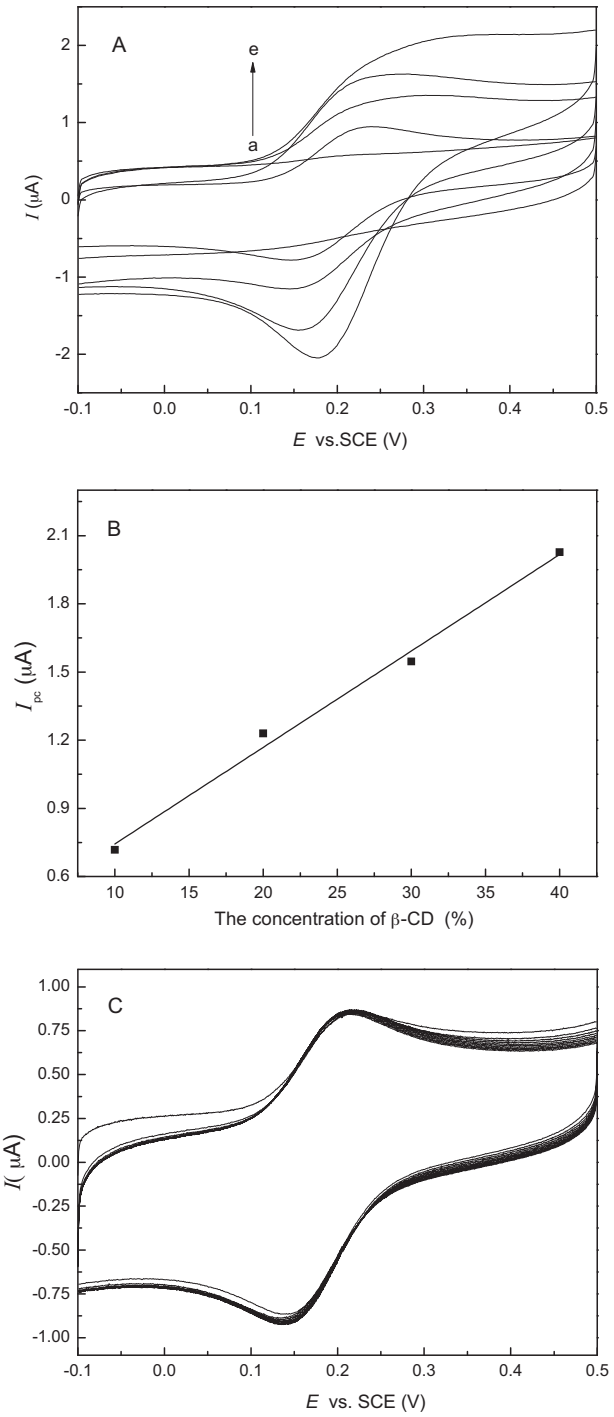

Fig. 5. (A) The cyclic voltammograms of Fc absorbed by β-CD/PVA_{nfm} with at different concentrations modified electrode in 0.1M PBS (pH 6.8), T = 25 °C, ν = 0.1 V s^{-1}: (a) 0 wt.%, (b) 10 wt.%, (c) 20 wt.%, (d) 30 wt.%, (e) 40 wt.%. (B) The cathodic peak current as a function of β-CD concentration. Date taken from (A). (C) The multi-cyclic voltammograms of Fc absorbed by β-CD/PVA_{nfm} (β-CD, 10 wt.%) modified electrode in 0.1 M PBS (pH 6.8), T = 25 °C, ν = 0.1 V s^{-1}.

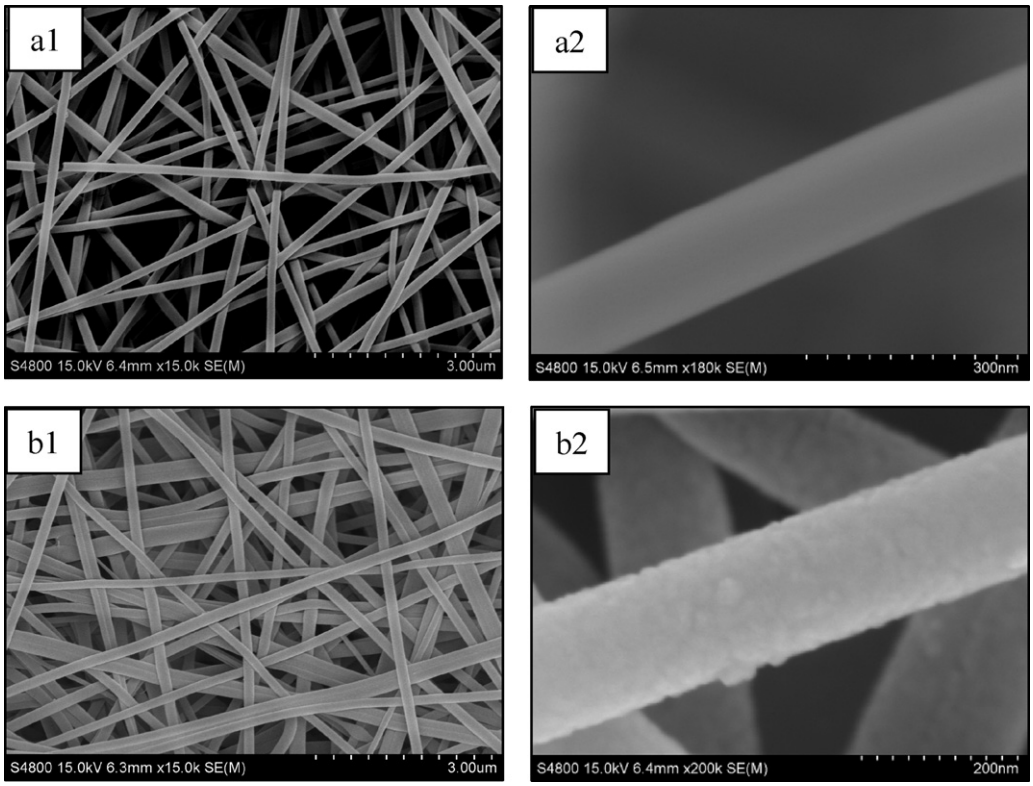

Fig. 6. SEM images of the β-CD/PVA_{nfm} (30 wt.% β-CD) modified electrode before (a1 and a2) and after capturing the Fc (b1 and b2).

4. Conclusion

In the present work, β-CD/PVA_{nfm} was successfully prepared by electrospinning of PVA solutions with different addition of β-CD. Fiber diameters were increased with the concentration of β-CD. The morphology of electrospinning fibers strongly depended on the viscosity of β-CD/PVA solutions, which was due to the hydrogen bonding between β-CD and PVA. According to electrochemical methods, moreover, we demonstrated that the electrospinning uniform β-CD/PVA_{nfm} could capture some organic molecule readily and effectively. Since the composite nanofibrous membrane could be used as the attractive host matrix for the available loading of guest molecules in the modified electrode and result in the enhanced electrochemical response. Thus, the specific property of β-CD functional nanofibrous membrane, in the case of supermolecule interactions, would be exploited and combined with electrochemical detections and biocatalysis.

Acknowledgments

The authors acknowledged the financial support from the National Natural Science Foundation of China (Grant Nos. 20773107, 20973151, and 20901065), the Natural Science Key Foundation of Educational Committee of Jiangsu Province of China (Grant No. 07KJA15015), the Specialized Research Fund for the Doctoral Program of Higher Education (SRFDP, 20093250110001), and the Foundation of Jiangsu Provincial Key Program of Physical Chemistry in Yangzhou University.

References

Barhate, R. S., & Ramakrishna, S. (2007). Nanofibrous filtering media: Filtration problems and solutions from tiny materials. *Journal of Membrane Science*, *296*, 1–8.

Buriez, O., Heldt, J. M., Labbé, E., Vessières, A., Jaouen, G., & Amatore, C. (2008). Reactivity and antiproliferative activity of ferrocenyl-tamoxifen adducts with cyclodextrins against hormone-independent breast-cancer cell lines. *Chemistry – A European Journal*, *14*, 8195–8203.

Chen, M., Diao, G., & Zhang, E. (2006). Study of inclusion complex of β-cyclodextrin and nitrobenzene. *Chemosphere*, *63*, 522–529.

Fong, H., Chun, I., & Reneker, D. H. (1999). Beaded nanofibers formed during electrospinning. *Polymer*, *40*, 4585–4592.

Gholap, S. G., Jog, J. P., & Badiger, M. V. (2004). Synthesis and characterization of hydrophobically modified poly(vinyl alcohol) hydrogel membrane. *Polymer*, *45*, 5863–5873.

Greiner, A., & Wendorff, J. H. (2007). Electrospinning: A fascinating method for the preparation of ultrathin fibers. *Angewandte Chemie International Edition*, *46*, 5670–5703.

Jia, Y. T., Gong, J., Gu, X. H., Kim, H. Y., Dong, J., & Shen, X. Y. (2007). Fabrication and characterization of poly(vinyl alcohol)/chitosan blend nanofibers produced by electrospinning method. *Carbohydrate Polymers*, *67*, 403–409.

Jozefaciuk, G., Muranyi, A., & Fenyvesi, E. (2003). Effect of randomly methylated β-cyclodextrin on physical properties of soils. *Environmental Science & Technology*, *37*, 3012–3017.

Li, S., & Purdy, W. C. (1992). Cyclodextrins and their applications in analytical chemistry. *Chemical Reviews*, *92*, 1457–1470.

Li, D., & Xia, Y. N. (2004). Electrospinning of nanofibers: Reinventing the wheel? *Advance Materials*, *16*, 1151–1170.

Matsue, T., Evans, D. H., Osa, T., & Kobayashi, N. (1985). Electron-transfer reactions associated with host–guest complexation. Oxidation of ferrocenecarboxylic acid in the presence of β-cyclodextrin. *Journal of the American Chemical Society*, *107*, 3411–3417.

Namazi, H., & Kanani, A. (2009). Investigation diffusion mechanism of β-lactam conjugated telechelic polymers of PEG and β-cyclodextrin as the new nanosized drug carrier devices. *Carbohydrate Polymers*, *76*, 46–50.

Otsubo, Y. (1995). Rheology control of suspensions by soluble polymers. *Langmuir*, *11*, 1893–1898.

Reneker, D. H., & Yarin, A. L. (2008). Electrospinning jets and polymer nanofibers. *Polymer*, *49*, 2387–2425.

Shan, D., Qian, B., Ding, S. N., Zhu, W., Cosnier, S., & Xue, H. G. (2010). Enhanced solid-state electrochemiluminescence of Tris(2,2′-bipyridyl) ruthenium(II) incorporated into electrospun nanofibrous mat. *Analytical Chemistry*, *82*, 5892–5896.

Szejtli, J. (1998). Introduction and general overview of cyclodextrin chemistry. *Chemical Reviews*, *98*, 1743–1753.

Uyar, T., Kingshott, P., & Besenbacher, F. (2008). Electrospinning of cyclodextrin-pseudopolyrotaxane nanofibers. *Angewandte Chemie International Edition*, *47*, 9108–9111.

Uyar, T., Balan, A., Toppare, L., & Besenbacher, F. (2009). Electrospinning of cyclodextrin functionalized poly(methyl methacrylate) (PMMA) nanofibers. *Polymer*, *50*, 475–480.

Wang, X., Chen, X., Yoon, K., Fang, D., Hsiao, B. S., & Chu, B. (2005). High flux filtration medium based on nanofibrous substrate with hydrophilic nanocomposite coating. *Environmental Science & Technology*, *39*, 7684–7691.

Xu, F., Zhang, Z., Ping, Y., Li, J., Kang, E., & Neoh, K. (2009). Star-shaped cationic polymers by atom transfer radical polymerization from β-cyclodextrin cores for nonviral gene delivery. *Biomacromolecules*, *10*, 285–293.

Yang, Y., Gu, Z., Xu, H., Li, F., & Zhang, G. (2010). Interaction between amylose and β-cyclodextrin investigated by complexing with conjugated linoleic acid. *Journal of Agricultural and Food Chemistry*, *58*, 5620–5624.

Yu, Y., Gu, L., Zhu, C., Aken, P. A., & Maier, J. (2009). Tin nanoparticles encapsulated in porous multichannel carbon microtubes: Preparation by single-nozzle electrospinning and application as anode material for high-performance Li-based batteries. *Journal of the American Chemical Society*, *131*, 15984–15985.

Zhao, J., Lin, D., Wang, Y., & Yao, S. (2010). A novel β-cyclodextrin polymer/tungsten carbide composite matrix for expanded bed adsorption: Preparation and characterization of physical properties. *Carbohydrate Polymers*, *80*, 1085–1090.